# A Shadow of the Extragalactic X-Ray Background

Joel N. Bregman – University of Michigan
Jimmy A. Irwin – University of Michigan



Citation of published version:

Bregman, J., Irwin, J. (2002): A Shadow of the Extragalactic X-Ray Background. *The Astrophysical Journal Letters*, 565(1). DOI: 10.1086/339244

THE ASTROPHYSICAL JOURNAL, 565:L13–L16, 2002 January 20


# A SHADOW OF THE EXTRAGALACTIC X-RAY BACKGROUND

JOEL N. BREGMAN AND JIMMY A. IRWIN
Astronomy Department, University of Michigan at Ann Arbor, 830 Dennison,
501 East University Avenue, Ann Arbor, MI 48109-1090
*Received 2001 July 27; accepted 2001 December 17; published 2002 January 9*

## ABSTRACT

The majority of baryons in the local universe are expected to lie outside of galaxies, in modest overdensity regions of the universe. This gas is predicted to be at a temperature of $10^5$–$10^7$ K and to emit X-rays that can contribute significantly to the X-ray background near 0.75 keV. If present, the gas in an edge-on galaxy would absorb this diffuse background emission, causing a shadow. We carried out this test using *Chandra* observations of the edge-on galaxy NGC 891 and using a cool, gas-rich region defined by high optical extinction, and we detect a shadow in the 0.4–1.0 keV band at the 99% confidence level. This shadow corresponds to approximately one-half of the total X-ray background in this energy range, brighter than the mean predicted value for emission from diffuse baryons but within the range of model values.

*Subject headings:* diffuse radiation — galaxies: individual (NGC 891) — intergalactic medium — X-rays: galaxies

## 1. INTRODUCTION

An inventory of the baryons at the present epoch shows that the visible galaxies, cold gas, and the hot gas in clusters and rich groups comprise only about 20% of the baryons inferred from big bang nucleosynthesis (Fukugita, Hogan, & Peebles 1998; Cen & Ostriker 1999a). Most of the baryons must be in a form that is difficult to detect, and cosmological simulations suggest that they are still in the gaseous phase in regions of low and moderate overdensities ($\rho/\Delta\rho = 10$–$100$; Cen et al. 1995; Cen & Ostriker 1999a, 1999b; Croft et al. 2001). In the simulations, gravitational collapse leads to compressional and shock heating of the gas, generating temperatures of $10^5$–$10^7$ K, at which hydrogen is completely ionized. The metallicity of the gas is estimated to be about 0.1–0.2 of the solar value, leading to X-ray line emission (e.g., from Fe and O), which when summed over many filaments and large volumes, is predicted to be detectable as a diffuse X-ray background (XRB), comprising about 10%–35% of the XRB in the 0.5–1 keV range (Cen & Ostriker 1995, 1999a), with large spatial variation (Croft et al. 2001). The detection of this diffuse extragalactic background would represent the first evidence for the expected "missing" baryons.

Separating this component from an X-ray observation is a considerable challenge because a typical image also consists of emission from an ensemble of point sources (mainly active galactic nuclei [AGNs]), a diffuse instrumental background, and a diffuse Galactic background. One of the best techniques for isolating the diffuse extragalactic XRB component is through X-ray shadowing of the background by a cold gas cloud (e.g., Warwick & Roberts 1998). Since it is extremely rare to find neutral extragalactic gas clouds with moderate X-ray optical depths, here we use the gas within an edge-on spiral galaxy, where the large column density ($10^{21}$–$10^{22}$ cm$^{-2}$) can make a deep shadow at soft energies ($E < 1$ keV).

The edge-on galaxy used in this study is the fairly isolated system NGC 891 ($d = 10$ Mpc), a nearby spiral galaxy similar to the Milky Way that is rich in neutral gas and shows strong optical extinction in the midplane. This galaxy has been observed in a wide range of wave bands, including *ROSAT*, which showed that it has extended X-ray emission as well as point sources in the plane; these issues must be dealt with in the analysis of the shadow (Bregman & Pildis 1994; Bregman & Houck 1997).

## 2. OBSERVATIONS AND DATA PROCESSING

Observations were obtained on 2000 November 1–2 with the back-side–illuminated S3 chip on the ACIS-S array, as this provides the greatest sensitivity at soft energies. The center of NGC 891 was located at the center of the S3 chip, 1.′757 from the location of best focus, and with the galaxy oriented diagonally across the square detector. The total exposure time was 51 ks, but an analysis of the background as a function of time revealed a period of high background due to charged particles, so we excluded data where the background was 1.3 above the modal value of the background. After this filtering, 36 ks of data remained and only the standard good grade ACIS events were used. Level 1 and level 2 data products were produced with ASCDS version R4CU5UPD11.1 of the processing software; subsequent processing was carried out with CIAO version 2.1.

We flattened the image with the exposure map for the S3 chip. Point-source identification was carried out using the energy band 0.5–6 keV, because above 6 keV the background rises rapidly, while below 0.5 keV there are few additional counts from point sources and the background also becomes brighter. We identified point sources both by eye and by using the task WAVDETECT, which gives an estimate of the error. Both approaches led to identical source lists, although we calculated our own determination of the probability that the source was a random Poisson fluctuation by using the point-spread function at the location of a target (50% and 90% encircled energies) and the local value of the background from WAVDETECT. We retained a source if the probability of it being a random fluctuation was less than 0.1; $A/1024^2$, where $A$ is the area of the point-spread function in pixels for the full-resolution image (1024 pixels on a side). This approach should lead to fewer than one false detection on the field.

The detection threshold for point sources varies modestly across the S3 chip because within 2.′5 of the aimpoint, a source is defined by only five photons, while at 6′ from the aimpoint, a source is defined by nine photons (50% encircled energy); the detection efficiency is slightly lower when using the 90%

FIG. 1.—The 0.4–1.0 keV ACIS-S *Chandra* image of NGC 891 (5′ : 18″ high by 6′ : 20″ wide, with 0.″5 pixels). Many of the point sources are in NGC 891, either just above or below the plane, with a central shadow created by the absorbing disk gas.

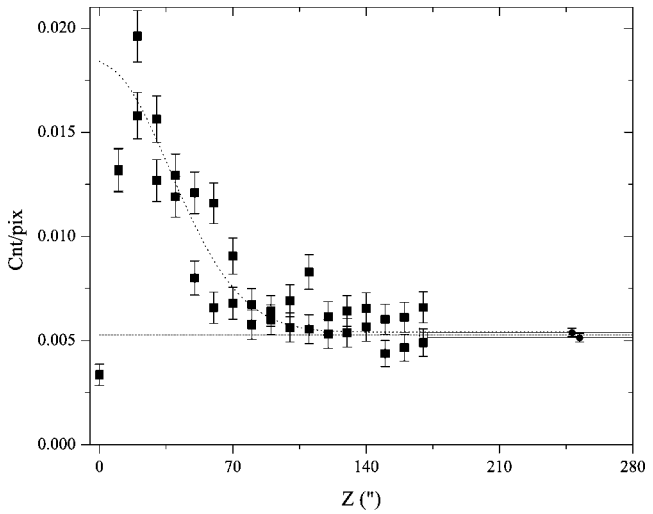


FIG. 2.—Surface brightness distribution of the diffuse emission in the NGC 891 field. The emission perpendicular to the disk of NGC 891 (in *z*) was determined in long rectangles (10″ × 4′) for both sides of the disk (folded here), except for the midplane region (shown in Fig. 3) and the outer background region, which are larger polygons (*solid circles with vertical error bars and a horizontal bar showing spatial extent*). The horizontal dashed line is the mean of the two backgrounds, extended back to $z = 0$ so that one can see the difference between the background and the shadow (at $z = 0$). All point sources are removed. The Gaussian fit to the *ROSAT* data, scaled to the *Chandra* image, is shown as a dotted line.

encircled energy. For the northwest region of the chip that we use to define the background, the detection limit is 4–5 photons, while in the southeast region used to define the background, the detection limit is 6–7 photons (50% encircled energy). In averaging the two background regions and correcting the detections to 100% enclosed energy, we find an average detection limit is 11 photons. For a power-law spectral energy distribution with a photon index of $\Gamma = 1.4$ and Galactic absorption of $7 \times 10^{20}$ cm$^{-2}$, 11 photons (a rate of $3.04 \times 10^{-4}$ counts s$^{-1}$) is equal to $2.09 \times 10^{-15}$ ergs cm$^{-2}$ s$^{-1}$ in the 0.5–6 keV band, or $7.87 \times 10^{-16}$ ergs cm$^{-2}$ s$^{-1}$ in the 0.5–2 keV band and $3.1 \times 10^{-16}$ ergs cm$^{-2}$ s$^{-1}$ in the 0.5–1 keV band (all fluxes are absorption corrected).

## 3. EXTENDED EMISSION AND ABSORPTION FEATURES

Previous X-ray observations of NGC 891 with *ROSAT* revealed several point sources as well as extended emission, both along and perpendicular to the plane (Bregman & Pildis 1994; Bregman & Houck 1997). Many additional point sources are found in the *Chandra* image (Fig. 1), with the two brightest being in the disk: SN 1986J and the luminous point source 27″ from SN 1986J (to be discussed in a future work).

The extent of the diffuse emission perpendicular to the disk was quantified by determining the surface brightness distribution in the 0.4–1.0 keV band, excluding point sources, and in long, thin boxes (4′ long by 10″ high) aligned parallel to the disk at increasing distances from the disk (Fig. 2). The diffuse emission extends about 100″ perpendicular to the disk, which was also found with the *ROSAT* data by Bregman & Houck (1997), who fit the distribution with a Gaussian of $\sigma = 37''$. Beyond 100″ and to the location of the inner support ring of the Position Sensitive Proportional Counter (PSPC; 17′), the *ROSAT* data showed no additional emission or deviations from flatness in the field, which is consistent with these *Chandra* data.

The most striking aspect of the 0.4–1.0 keV image is the local minimum in the central disk of the galaxy, which is evident to the eye and is about 10″–15″ wide and several arcminutes long. Since there is diffuse emission around the galaxy, this local minimum is accentuated, so the question is whether this local minimum falls below the background in the field defined away from diffuse emission of NGC 891. Although the eye identifies the shape of the local minimum, we wanted a more objective means of defining this region. Unfortunately, the spatial resolution of the direct tracers of cold gas, such as an H I or a far-infrared dust map, are too coarse (Swaters, Sancisi, & van der Hulst 1997). We need a measure of the column of gas in front of most of the stellar light, since this is the gas that is creating the local minimum, and the best available tracer is the extinction against the starlight. The extinction is not symmetric about the center of the galaxy, with more extensive extinction toward the south, the side to which the H I is more extended. The *V*-band image was used to create a region boundary that encompassed an area of substantial extinction, shown superposed on Figure 3 (we obtain the same region from *B*- and *R*-band images). In producing this boundary, we sought a minimum contrast of a factor of 2 between the bright disk and the adjacent extinguished disk. This is a sensible but is not a unique choice that leads to an extinction region about 0.6 kpc thick vertically, about the FWHM of H I in the Milky Way, which is similar to NGC 891. The extinction region comprises 10,923 pixels (0.″5 on a side), or 0.735 arcmin$^2$. We note that even at this extinction level, not all of the emission from a disk would be absorbed in the 0.4–1 keV band.

The X-ray surface brightness within the extinction region is 0.0036 counts pixel$^{-1}$ (0.″5 pixels) compared to the background value of $0.00527 \pm 0.00014$ counts pixel$^{-1}$, or in numbers of photons, there were 39.5 photons in the extinction region, whereas 57.6 were expected to be present, a deficit of 18.1 ($+6.5$, $-5.6$) photons (an effective 1 $\sigma$ error based on 39.5 photons). Using Poisson statistics, the probability that this deficit occurred by chance is 1%. We consider this result significant because we determined the location of the expected shadow and its energy band *before* the observations were obtained.

It is not possible to determine the spectral properties of the

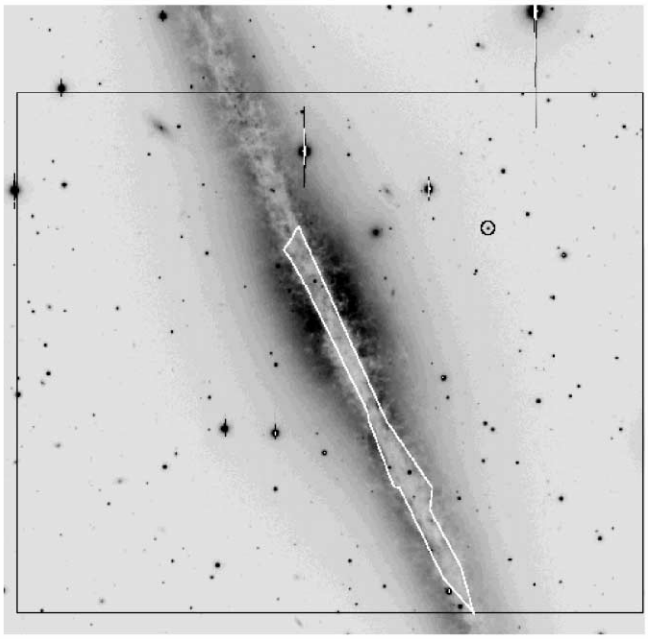

FIG. 3.—*V*-band image of NGC 891, from Howk & Savage (2000; 6′ : 20″ on a side), with an outline of a region of deep extinction that was used as the extraction region in determining the depth an significance of the X-ray shadow. The black outline of a rectangle is the *Chandra* image shown in Fig. 1, and the circled point source to the northwest of the galaxy center corresponds to the bright X-ray point source in the same location in Fig. 1.

diffuse background from 18 photons, although the "missing" photons are distributed in energy from 0.4–1.0 keV and are not clumped at a single energy region, consistent with the expectations for a shadow of a diffuse extragalactic component. Also, although we used the 0.4–1.0 keV band (chosen before the analysis was begun), the significance of the shadow can be increased by choosing a slightly different energy band or different time-filtering limits or by drawing the shadow region subjectively. At energies above about 1.5 keV, the opacity through the disk decreases, and we begin to see the multitude of disk X-ray binary sources, so the disk is becoming a source of net emission, as expected.

There are no known instrumental effects that would lead to this result, and the only unresolved instrumental issues would deepen the shadow. We have examined other observations taken with the S3 chip in the same chip locations and found no evidence of a local minimum. Another issue is the flatness of the field, where corrections by the exposure map were modest except near the chip boundaries, which were not used. Studies of field flatness show that the field often does not flatten completely; i.e., the background turns down toward the edges of the chip by up to 30% in the 5–10 keV band (on-line *Chandra* documentation). We see this effect in these data in the 2–6 keV range, where the shadow is unimportant, and if it occurs in the 0.4–1.0 keV range, then we have *underestimated* the depth of the shadow, as we would be using a background value in the field that is too low.

## 4. INTERPRETATION OF THE SHADOW

There are several components that can contribute to the X-ray emission in this energy range: diffuse emission from the gas in or near the Milky Way, emission from the AGNs that dominate the resolvable XRB, a diffuse extragalactic background due to hot gas, and the instrumental background (Table 1; the second column is the absorption-corrected emission, while the third column is the number of observed photons with no absorption correction). We discuss the contribution of components in directions of low Galactic contribution to the background and explain how this particular region differs.

In the 0.1–2 keV band, the background emission has been mapped with *ROSAT* (Snowden et al. 1997) in discrete bands, of which the R4 (0.52–0.69 keV) and R5 (0.70–0.90 keV) bands are closest to our 0.4–1.0 keV band. In these bands, the diffuse emission within 2° of NGC 891 is about 20% above the typical rates at high Galactic latitudes. Toward a typical high-latitude region, McCammon et al. (2001) obtained microcalorimeter spectra and detected low-redshift O VII and O VIII emission lines presumably due to the Milky Way. The power in these lines plus the continuum constitute about 38% of the R4 flux and 15% of the R5 flux, or about 25% of the total XRB in the 0.4–1.0 keV band.

The AGN component constitutes a bit less than half of the XRB in this energy band, although there is some uncertainty (Hasinger et al. 1998; Mushotzky et al. 2000; Giacconi et al. 2001; Gilli, Salvati, & Hasinger 2001; Brandt et al. 2001). The total AGN contribution is usually determined by extrapolating the 2–10 keV background to lower energies. Unfortunately, different experiments obtain somewhat different values for the absolute level of the background in this region, ranging from $8E^{-0.4}$ to $11E^{-0.4}$ keV cm$^{-2}$ s$^{-1}$ sr$^{-1}$ keV$^{-1}$ (review by McCammon & Sanders 1990). To our point-source limit, we resolve at least 72%–84% of the AGN contribution, although it is probably more appropriate to use a model to extrapolate the power-law spectrum to lower energies. When we use the fast evolution model of Gilli et al. (2001), scaled to the higher value of the background (the result is unchanged if we use their slow evolution model), we have resolved at least 80% of the AGN background, or an unresolved flux of 1.2 keV cm$^{-2}$ s$^{-1}$ sr$^{-1}$. However, sources comparable to and fainter than our detection limit are generally self-absorbed, which produces the flatter spectra necessary to account for the shape of the 2–10 keV XRB (Hasinger et al. 1998; Giacconi et al. 2001; Gallagher et

TABLE 1

AMOUNTS OF THE X-RAY COMPONENTS IN 0.4–1.0 keV

| Component | Total X-Ray Background (keV cm$^{-2}$ s$^{-1}$ sr$^{-1}$) | Diffuse Image Emission (photons) |
|---|---|---|
| Instrumental background ..... | ... | 20–30 |
| Shadow component ..... | 17.5 | 18.1 (+6.5, −5.6)[a] |
| AGN ..... | 6.3[b] | ... |
| Milky Way emission ..... | 4–8 | 6–12 |
| Total ..... | 16–31 | 57.6 |

[a] Shadow component is the sum of the diffuse extragalactic component plus a minor contribution (2%–7%) from unresolved AGNs.

[b] Unresolved AGN component is 0.3–1.2 keV cm$^{-2}$ s$^{-1}$ sr$^{-1}$.

al. 2001; Brandt et al. 2001). If the remaining 20% of the unresolved AGNs are self-absorbed with a power-law spectrum of $\Gamma = 1.7$ and an absorbing column of $10^{22}$ cm$^{-2}$ with a 90% covering factor (after Gallagher et al. 2001), the diffuse unresolved AGN background is 0.3 keV cm$^{-2}$ s$^{-1}$ sr$^{-1}$. Therefore, the unresolved AGN component accounts for only 2%–7% of the total 0.4–1.0 keV XRB, and even at the maximum possible value (1.2 keV cm$^{-2}$ s$^{-1}$ sr$^{-1}$), it is far too small to account for the observed shadow (17.5 keV cm$^{-2}$ s$^{-1}$ sr$^{-1}$; Table 1).

The remaining contribution to the background is the diffuse extragalactic XRB, originally estimated to contribute about one-quarter of the 0.4–1.0 keV background (Cen et al. 1995). However, calculations by Voit, Evrard, & Bryan (2001) and Croft et al. (2001) show that there will be considerable structure in the intensity of the diffuse extragalactic XRB, ranging from being a negligible contribution to being most of the XRB. The brighter regions correspond to emission from groups, while the faintest lines of sight have no collapsed structures of any significance.

The depth of the shadow corresponds to a flux, corrected for Galactic absorption, of 17.5 keV cm$^{-2}$ s$^{-1}$ sr$^{-1}$, assuming a power-law spectrum with a photon index of 1.5 (Table 1); for a thermal plasma at 20% solar metallicity, we obtain the same flux for $T = 10^{6.5}$ K and a 7% lower flux for $T = 10^{7}$ K. This flux associated with the shadow is comparable to the entire typical high-latitude XRB brightness. Given the value for the instrumental background (close to the nominal value discussed in *Chandra* documentation), the diffuse component of the XRB is locally higher at this location. The intensity associated with the shadow would require a value for the diffuse baryonic component that is brighter than average and occurs for ~10% of the sky (Voit et al. 2001).

In addition, we considered whether NGC 891 lies in an X-ray–emitting group, in which case its gas is merely shadowing the back side of the emission from the group. The nearest comparable galaxy is NGC 1023, a spiral that is about 5° away (1 Mpc), which would make it a poor spiral group, and such systems are generally not X-ray emitters (Mulchaey 2000). Furthermore, no extended X-ray emission is seen in the field of the *ROSAT* PSPC out to 17′ (50 kpc), so if there is an extensive group emission, it would need to have an unusually large core radius. Nevertheless, we hope to examine this possibility with future observations.

## 5. FINAL COMMENTS AND FUTURE PROSPECTS

The "missing" baryons in the local universe are predicted to produce a diffuse XRB, which we have detected through a shadowing observation where the absorbing screen is the gaseous disk of the edge-on galaxy NGC 891. The depth of this shadow is consistent with, but at the high end of, the range of predicted intensities. Shadows have been seen at 0.25 keV with *ROSAT* (Warwick & Roberts 1998), but given the uncertainties, these shadows may arise entirely from unresolved AGNs, although a significant diffuse gaseous component could also be accommodated. Whereas our observation shows this to be a worthwhile area of investigation, there are many basic questions that still need to be addressed, such as the spectrum of the diffuse background, its variation in intensity with position on the sky, and its redshift distribution.

Our near-term goals are to improve the determination of the depth of the shadow in NGC 891 and to examine whether other parts of the sky show similar shadow depths, thereby addressing the prediction of intensity variation on the sky. However, measurement of the spectral shape of the diffuse background and of its redshift distribution is beyond the capabilities of either *Chandra* or *XMM* and will require an instrument with excellent spectral and spatial capabilities over moderate angular fields of view and with low instrumental background.

We thank the members of the *Chandra* Science Center for the assistance in understanding the many details of ACIS observations, with special thanks to Maxim Markavitch, Bill Forman, Christine Jones, and Larry David. Scientific guidance and assistance from Dan McCammon, Wilt Sanders, and Steve Snowden has been very valuable in interpreting our results. We thank Chris Howk for making available his optical data of NGC 891 and Renato Dupke for criticisms and comments. This work has been supported by the *Chandra* Guest Observer program through grant NASA GO0-1147X and through the *Chandra* Fellowship Program (for J. A. I.).

## REFERENCES

Brandt, W. N., et al. 2001, AJ, 122, 1
Bregman, J. N., & Houck, J. C. 1997, ApJ, 485, 159
Bregman, J. N., & Pildis, R. A. 1994, ApJ, 420, 570
Cen, R., Kang, H., Ostriker, J. P., & Ryu, D. 1995, ApJ, 451, 436
Cen, R., & Ostriker, J. P. 1999a, ApJ, 514, 1
———. 1999b, ApJ, 519, L109
Croft, R. A. C., di Matteo, T., Davé, R., Hernquist, L., Katz, N., Fardal, M. A., & Weinberg, D. H. 2001, ApJ, in press
Fukugita, M., Hogan, C. J., & Peebles, P. J. E. 1998, ApJ, 503, 518
Gallagher, S. C., Brandt, W. N., Laor, A., Elvis, M., Mathur, S., Wills, B. J., & Iyomoto, N. 2001, ApJ, 546, 795
Giacconi, R., et al. 2001, ApJ, 551, 624
Gilli, R., Salvati, M., & Hasinger, G. 2001, A&A, 366, 407
Hasinger, G., Burg, R., Giacconi, R., Schmidt, M., Trümper, J., & Zamorani, G. 1998, A&A, 329, 482
Howk, J. C., & Savage, B. D. 2000, AJ, 119, 644
McCammon, D., & Sanders, W. T. 1990, ARA&A, 28, 657
McCammon, D., et al. 2001, ApJ, submitted
Mulchaey, J. S. 2000, ARA&A, 38, 289
Mushotzky, R., Cowie, L. L., Barger, A. J., & Arnaud, K. A. 2000, Nature, 404, 459
Snowden, S. L., et al. 1997, ApJ, 485, 125
Swaters, R. A., Sancisi, R., & van der Hulst, J. M. 1997, ApJ, 491, 140
Voit, G. M., Evrard, A. E., & Bryan, G. L. 2001, ApJ, 548, L123
Warwick, R. S., & Roberts, T. P. 1998, Astron. Nachr., 319, 59